

Supplementary material and results

***In situ* matured early-stage human induced pluripotent stem cell-derived cardiomyocytes improve cardiac function by enhancing segmental contraction in infarcted rats**

Author's list:

Diogo Biagi ¹, Evelyn Thais Fantozzi ^{1, #}, Julliana C Campos-Oliveira ^{1, #}, Marcus Vinicius Naghetini ^{1, #}, Antonio F. Ribeiro Jr. ^{1, #}, Sirlene Rodrigues ¹, Isabella Ogusuku ^{1, 2}, Rubia Vanderlinde ¹, Michelle Lopes Araújo Christie ³, Debora B. Mello ³, Antonio C. Campos de Carvalho ³, Marcos Valadares ¹, Estela Cruvinel ¹ and Rafael Dariolli ^{1, 4, *}

Affiliations:

¹*PluriCell Biotech, 05508-000, São Paulo, SP, Brazil*

²*Gene Center and Department of Biochemistry, Ludwig-Maximilians-Universität München, 81377, München, Germany*

³*Carlos Chagas Filho Institute of Biophysics, Federal University of Rio de Janeiro, Rio de Janeiro, 21941-902, Brazil*

⁴*Department of Pharmacological Sciences, Icahn School of Medicine at Mount Sinai, 10029, New York, NY, USA*

These authors equally contributed to this work

** rafael.dariolli@mssm.edu*

Table of Contents

Supplementary Experimental Procedures	3
Cardiomyocytes derived from human induced pluripotent stem cells (hiPSC-CM)	3
Flow cytometry	4
Immunocytochemistry	4
Permanent coronary artery occlusion – myocardial infarction- Induction	4
Echocardiographic assessments.....	5
LVEF pre-injection-based exclusion Criteria.....	6
Anatomopathological injury assessments	7
Human Ku80 positive graft assessments	8
Biodistribution.....	9
References.....	10
Table S1: LVEF distribution in MI-induced rats after randomization.....	11
Table S2: Percentage of hKu80 positive versus scar tissue area per animal.	11
Table S3: Antibodies list.....	12
Table S4: List of reagents used in this study.	13
Supplementary Figures	14
Figure S1: <i>Bodyweight control and survival rate</i>	14
Figure S2: <i>MI area and LVEF pre-injections</i>	15
Figure S3: <i>Short Axis Strain Analysis</i>	16
Figure S4: <i>Long Axis Strain Analysis</i>	17
Figure S5: <i>Morphology of the human graft</i>	18
Figure S6: <i>Maturation and cell-cell interaction</i>	19
Figure S7: <i>Immunofluorescence staining for TNNT2 and Pan-cadherin</i>	20
Figure S8: <i>Immunofluorescence staining for TNNT2 and Cx43</i>	21
Figure S9: <i>Immunofluorescence staining for TNNT2 and Caveolin 3</i>	22
Figure S10: <i>Flow Cytometry quality-control analysis for monitor hiPSC-CMs maturation over time</i>	23
Figure S11: <i>Immunohistochemistry for inflammatory markers</i>	24
Figure S12: <i>Human mitochondrial DNA was identified in some tissues</i>	25
Figure S13: <i>Necropsy</i>	26

Supplementary Experimental Procedures

Cardiomyocytes derived from human induced pluripotent stem cells (hiPSC-CM)

ACP5 hiPSC, an *PluriCell Biotech* cell line, was expanded in feeder-free conditions using Essencial 8 medium (E8; Thermo Fisher Scientific, USA) until they reached 60–70% confluence. Cells were dissociated and plated (2.5×10^5 cells/cm²) with a 3:1 (vol/vol) mixture of E8 and StemFlex media (Thermo Fisher Scientific, USA) supplemented with 10 μ M Y-27632 (Cayman Chemical, USA). After 2 days, at day 0 of differentiation, the medium was changed to RPMI supplemented with 0.25X B27 supplement (Thermo Fisher Scientific, USA) without insulin (RB-) and 3 μ M CHIR99021 (Merck Millipore Sigma, USA). 24 hours later, 50% of the medium was changed to RB- supplemented with 20ng/mL BMP4 (R&D Systems, USA). On days 2 and 4, the medium was changed to fresh RPMI supplemented with 0.25X B27 supplement (Thermo Fisher, USA) (RB+) supplemented with 2 μ M KY2111 and 2 μ M XAV939 (both from Cayman Chemical, USA). On days 5 and 7, the medium was changed to fresh RPMI supplemented with 213 μ g/mL Ascorbic Acid (Sigma-Aldrich, USA), 500 μ g/mL BSA (CDM3). On day 8, cells were cultivated with RPMI without glucose (Thermo Fisher Scientific, USA) for three days. On day 10, media was changed to CDM3, and cells were cultivated until the day before the passage for injection, when they went through the Heat Shock process.

During the Heat Shock procedure, cultures were subjected to a 30min exposure to 43°C in medium RB+ supplemented with 100 ng/mL IGF-1 (PeproTech; USA) and 0.2 μ M cyclosporine A (Sigma-Aldrich; USA), followed by a return to a 37°C medium. Twenty-four hours later, cells were enzymatically isolated with 0.25U/mL Dispase and 0.5mg/mL collagenase II (Both from Sigma-Aldrich, USA) for 1 hour. The membranes were collected centrifuged and further digested with Accutase (Thermo Fisher Scientific, USA). After dilution in 1x HBSS with 1% Fetal Bovine

Serum (Thermo Fisher Scientific, USA) cells were counted and aliquoted in tubes with 10 million cells and kept at 10°C until the time of the syringe preparation.

Flow cytometry

Cells were fixed in 4% PFA (LabSynth, Brazil) and kept in the refrigerator for 3-7 days. Protein expression was analyzed by Flow Cytometry (FC) using antibodies for TNNT2, NKX2.5, MLC2V, MLC2A, TNNI1 and TNNI3 listed in Table S3. Data was acquired using CantoII BD equipment and analyzed by FlowJo Software considering 1-2% of false-positive events.

Immunocytochemistry

iPSC-CM were plated in 96-well plates coated with GELTREX for immunostaining. Cells were also fixed with 4% PFA (LabSynth, Brazil) and permeabilized with Triton 0.1% and Saponin 0.1% (both from Sigma-Aldrich, USA). Next, cells were stained with antibodies for TNNT2, NKX2.5, MLC2V, MLC2A listed in Table S3. All images were generated in EVOS FL (Thermo Fisher Scientific, USA).

Permanent coronary artery occlusion – myocardial infarction- Induction

Acute myocardial infarction was induced by permanent occlusion of the left anterior descending coronary artery as described previously with slight modifications [1]. Adult female Wistar rats weighing 150-200 grams were used. After anesthetized these animals were intubated by a cricothyroidotomy procedure and coupled to a mechanical respirator (tidal volume of 2.5mL, respiratory rate of 90-100 irpm). The animals underwent the following surgical procedure: skin incision at the left parasternal level, approximately 1cm long, located 1cm from the mid sternal line, at the junction of the lower and middle thirds between the collarbone and the costal margin. Then, the pectoral muscles, larger and smaller, were dissected aiming at the visualization of the left costal grating. At this time, a purse-string suture of the skin and muscles of the region was

made, leaving the knot open until the end of the surgery. With the aid of hemostatic forceps, the incision was made between the 4th and 5th left intercostal space, where the heart was then externalized through the passage and traction of 7-0 prolene thread through the apical region. At this point, the pericardium surrounding the heart was excised. So, the left coronary artery (usually under the left atrium) was permanently occluded with 7-0 prolene thread as close as possible to its origin in the aorta. Then the heart was quickly repositioned to its original anatomical site and the pouch suture knot finally tightened. The groups were randomized after the induction of myocardial infarction. The sham-operated group (SHAM) underwent the same surgical stress, but without coronary artery occlusion.

Echocardiographic assessments

In order to assess cardiac function, all the animals in this study were subjected to echocardiography pre- and post-treatments (On days 6 and 37 after MI-induction). Parasternal-long and short axis images were captured using VEVO 2100 ultrasound equipment (VisualSonics Vevo® 2100 Imaging System, Canada) with a MS250 transducer (14-24 MHz). Analyzes were performed *off-line* using Vevo-LAB (VisualSonics, Canada). Parameters such as Systolic and Diastolic volumes, were calculated using *Modified Simpson Algorithm* present in the Analysis software (parasternal-short axis sequential imaging from base to apex). Based on these volumes, the left ventricle ejection fraction (LVEF, %) was calculated pre- and post-injection treatments (On days 6 and 37 after MI induction). Also, linear measurements were obtained from parasternal-short and -long axis images. Left ventricle shortening fraction (LVSF, %) was calculated, using systolic and diastolic diameters. Still, left ventricle mass (LV mass, mg) was estimated by linear measurements. The beating rate (beats per minute – BPM) was calculated directly by animal table-ECG system connected to VEVO 2100 system. Echocardiographic results were interpreted

considering the American Society of Echocardiography recommendations [2] concerning the rat model. All parameters were shown as the mean values of three consecutive cardiac cycles. Transthoracic echocardiography image acquisition and analysis were performed by 2 experts blinded to the experimental groups.

In addition, Speckle-Tracking analyses to access LV radial, circumferential and longitudinal strains were performed using B-mode short- and long-axis 300 frames images using Vevo Strain Analysis Software (Vevo LAB - VisualSonics, Canada). The analysis was performed following the manufacture's user guide. Mean Strain Time-to-Peak (AVG PK %) was used as one of the proxies of strain. This parameter was assessed on both short- and long- axis images for radial and circumferential, and radial and longitudinal strain respectively. Also, Global Circumferential Strain (GCS) and Global Longitudinal Strain (GLS) were calculated from short- and long-axis images, respectively. Short-axis analyses were performed at papillary-level and long-axis analyses at the medial portion of the parasternal long-axis image (where the entire LV can be observed in the presence of the mitral and aortic valves). All Strain analyses incorporated 3-5 consecutive cardiac cycles. Algorithm and equation details can be found in the manufacture's user guide.

LVEF pre-injection-based exclusion Criteria

Six days after MI induction rats were subjected to an echocardiographic assessment of cardiac. On-line analysis of the LVEF was performed by a technician and these results were used to randomize MI-induced rats in two groups, namely: PSC (placebo for cells that received injections of vehicle – pro-survival cocktail) and CELL (PSC (vehicle) + 10 million hiPSC-CMs). SHAM and CTRL animals were also imaged.

To investigate heart function improvement after cell injection into infarcted rats, we excluded from the analysis animals that had shown less than 20% decrease on LVEF when

compared to control animals (or up to 55% LVEF) indicating functional compromise after infarction. Due to a statistical difference observed between mean LVEF in the PSC and CELL groups after the randomization procedure, indicating a high level of heterogeneity in the injected group, we excluded animals of the cell injected group with LVEF below the minimum value observed in the PSC group, effectively balancing the two groups for direct comparison.

Anatomopathological injury assessments

Anatomic measurements were performed after the picrosirius red stain. This procedure consists of three steps, first the slides were deparaffinized with xylol (Êxodo Científica, Brazil) followed by a decreasing concentration battery of ethanol (Cirurgica Estilo, Brazil) solution washes. Then, slides were stained for 20min in Bouin fixative solution (Êxodo Científica, Brazil), washed in distilled water, and finally, the last bath with 0.1% Sirius red (Êxodo Científica, Brazil) in aqueous saturated picric acid solution (Imbralab, Brazil) was performed. Next, the slides were finalized using aqueous mount media (Vector, USA). To quantify injury perimeter and wall thickness on left ventricle ImageJ software was used as shown in **Figure** below. We measured the injury and healthy perimeters using the freehand selections tool of the software to calculate the percentage of injury (**Figure A**). For the wall thickness values, we have calculated the mean value of three different measurements with a straight-line tool from the injury and healthy areas (**Figure B**). In the same picrosirius stained slides, we also evaluated MI area and interstitial collagen using Image-Pro-Plus Software. To evaluate the area of injury, we first remove the right ventricle from the scanned 4x images with an image editor and then, we measured the percentage of injury by selecting the colors red (injury) and yellow (healthy) using the Count/Size tool (**Figure C**). A similar procedure was performed to measure interstitial collagen from 20 images taken at 20x in the injury and remote areas.

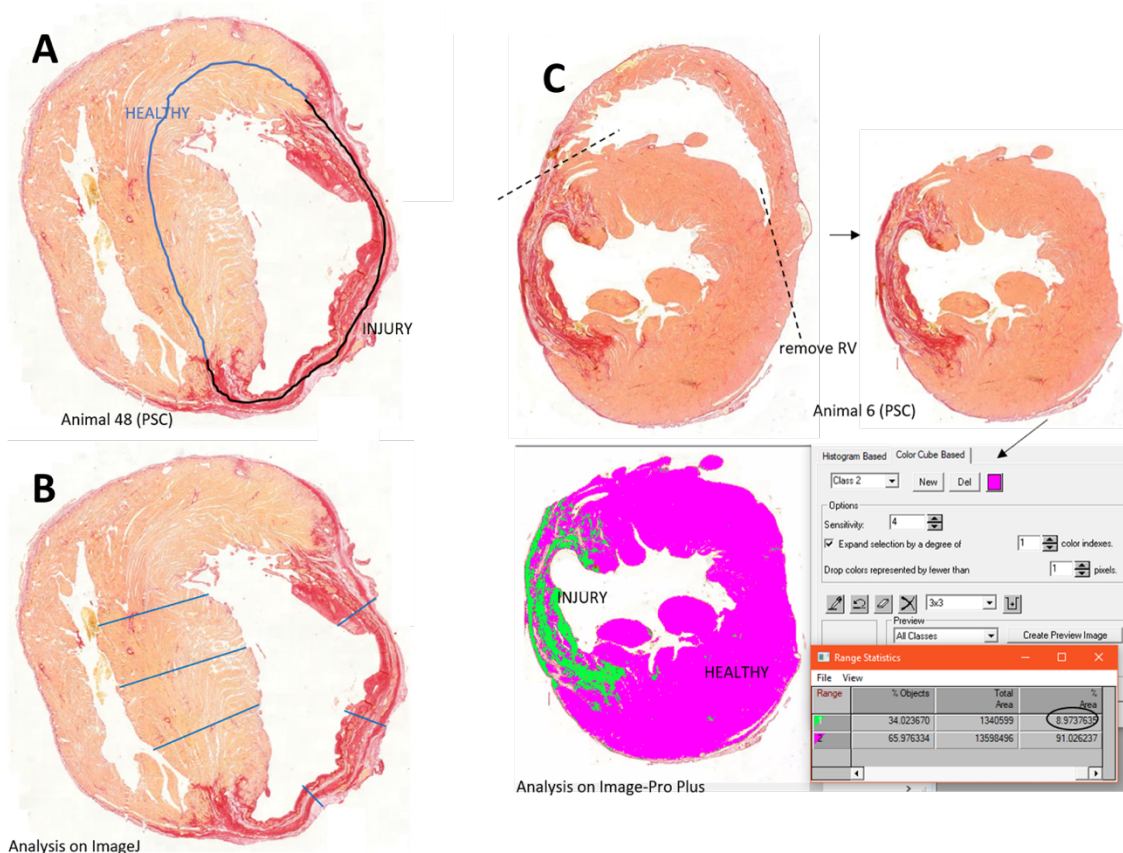


Figure: Examples of picrosirius red stain analysis. In A: perimeter area. In B: wall thickness. In C: injury area.

Human Ku80 positive graft assessments

To assess human graft tissues into the LV of injected rats, the sections were deparaffinized, then, heat-induced epitope retrieval was done with an electric pressure cooker for 15min, sections were quenched for unspecific binding with 5% donkey serum (Sigma, USA) + 0.5% TWEEN 20 in PBS (PBST) for 45min and incubated overnight at 4°C with primary antibody (antibodies list – Table S3). After 16 hours slides were washed with PBST and incubated with a secondary antibody (1:500) for 1h.

In IF, autofluorescence was blocked with a quenching kit (Trueview - Vector, USA). Finally, the slides were mounted using aqueous VectaShield media (Vector, USA) with DAPI. In IHC, the

reaction was amplified with avidin-biotin complex (Vector, USA) and revealed with DAB (Vector, USA). Counterstain was made with hematoxylin (Êxodo Cientifica, Brazil) for 5min. After immunostaining, the slides were mounted using aqueous media (Vector, USA).

Immunofluorescence and immunohistochemistry micrographs were obtained using TissueFAXS slide scanner (TissueGnostics, Austria), confocal microscope LSM 800 (Zeiss-Germany) and a conventional fluorescence microscope Axio Imager 2 (Zeiss-Germany). The analyses were performed using ImageJ through the multi-point tool used to count positive markers and nuclei and calculate the percentage of positive events.

Biodistribution

DNA was isolated from macerated liver, brain, lung, kidney, and spleen, and cryopreserved at -80°C from all animals using Wizard™ Genomic DNA Purification Kit (Promega, USA) following manufacturer's instructions. Then, end-point PCR was run with 200ng of all samples targeting human mitochondria: forward primer 5'-CACCGGCGCAGTCATTCTCATA-3' and reverse primer 5'-GAGTCCTGTAAGTAGGAGA-3' (265bp) [3]. It is worth mentioning that this primer pair also target human gDNA with the same product length, this causes no detriment in the analysis and most of the PCR products should be from mtDNA because their higher copy number per cell, but we cannot discriminate mtDNA from gDNA. Positive control reactions were done using 200ng of rat DNA supplemented with 10ng, 1ng, 100pg, 10pg, and 1pg of human DNA. Water was used as negative control and a rat specific Ahr sequence was also amplified: forward primer 5'-TGCCAGCAACAGCCTGTGAG-3' and reverse primer 5'-AACTGGCGAACATGCCATTGA-3' (650bp) [4]. PCR was analyzed by agarose gel electrophoresis (2% w/v).

All tissues that were positive for human DNA had 2 more DNA isolation performed from different sites from the same tissue sample. Moreover, quantitative PCR was run targeting mitochondrial sequence as described above. PCR was run in a QuantiStudio 3 Real-time system from Applied Biosystems. A standard curve of 200ng of rat DNA supplemented with 10ng, 1ng, 100pg, 10pg, and 1pg of human DNA was used and all samples were run in triplicates. Considering that a human cell DNA has 5pg of DNA [5], this assay can detect 1 human cell in 200.000 cells.

References

1. Olivares, E.L.; Ribeiro, V.P.; Werneck de Castro, J.P.S.; Ribeiro, K.C.; Mattos, E.C.; Goldenberg, R.C.S.; Mill, J.G.; Dohmann, H.F.; dos Santos, R.R.; de Carvalho, A.C.C.; et al. Bone marrow stromal cells improve cardiac performance in healed infarcted rat hearts. *Am. J. Physiol. Circ. Physiol.* **2004**, *287*, H464–H470, doi:10.1152/ajpheart.01141.2003.
2. Lang, R.M.; Bierig, M.; Devereux, R.B.; Flachskampf, F. a; Foster, E.; Pellikka, P. a; Picard, M.H.; Roman, M.J.; Seward, J.; Shanewise, J.S.; et al. Recommendations for chamber quantification: a report from the American Society of Echocardiography's Guidelines and Standards Committee and the Chamber Quantification Writing Group, developed in conjunction with the European Association of Echocardiograph. *J. Am. Soc. Echocardiogr.* **2005**, *18*, 1440–63, doi:10.1016/j.echo.2005.10.005.
3. Liu, Y.W.; Chen, B.; Yang, X.; Fugate, J.A.; Kalucki, F.A.; Futakuchi-Tsuchida, A.; Couture, L.; Vogel, K.W.; Astley, C.A.; Baldessari, A.; et al. Human embryonic stem cell-derived cardiomyocytes restore function in infarcted hearts of non-human primates. *Nat. Biotechnol.* **2018**, *36*, 597–605, doi:10.1038/nbt.4162.
4. Adamovic, T.; McAllister, D.; Guryev, V.; Wang, X.; Andrae, J.W.; Cuppen, E.; Jacob, H.J.; Sugg, S.L. Microalterations of Inherently Unstable Genomic Regions in Rat Mammary Carcinomas as Revealed by Long Oligonucleotide Array-Based Comparative Genomic Hybridization. *Cancer Res.* **2009**, *69*, 5159–5167, doi:10.1158/0008-5472.CAN-08-4038.
5. Sambrook, J. *Molecular cloning : a laboratory manual*; Third edition. Cold Spring Harbor, N.Y. : Cold Spring Harbor Laboratory Press, [2001] ©2001;

Supplementary Tables

Table S1: LVEF distribution in MI-induced rats after randomization.

Animal ID/details	Group/AVG	LVEF (pre-injection)
x	mean CTRL	68.6
x	cutoff	54.9
14	PSC	60.4
19	PSC	39.6
30	PSC	39.9
36	PSC	38.0
41	PSC	51.6
42	PSC	64.8
48	PSC	51.2
51	PSC	43.5
15	CELL	45.4
21	CELL	38.8
24	CELL	62.0
29	CELL	39.7
31	CELL	38.3
35	CELL	60.8
39	CELL	39.4
45	CELL	51.8
49	CELL	52.6
before cutoff	mean PSC	48.6
	mean CELL	47.6
after cutoff	mean PSC	44.0
	mean CELL	43.7

Table S2: Percentage of hKu80 positive versus scar tissue area per animal.

Animal ID	hKu80⁺ (mm²)	Injury (mm²)	% of human graft
15	0.18	4.78	3.62%
21	0.65	6.30	9.28%
29	0.99	3.96	19.93%
31	0.09	2.14	3.90%
39	0.14	9.50	1.44%
45	0.15	6.54	2.30%
49	0.14	4.21	3.12%

Table S3: Antibodies list for flow cytometry (FC), immunocytochemistry (ICC), immunohistochemistry (IHC) and histological immunofluorescence staining (IF). n/a means no apply.

Antibody	Procedure used and dilution	Company/catalogue number (#)	Retrieval buffer for IF
TNNI3	1:250 (IF)	Abcam/ab52862	Tris/EDTA pH 9.0
TNNI3	1:30 (FC)	DSHB/TI-4	n/a
TNNI1	1:500 (IF)	Thermo/701585	n/a
TNNT2	1:250 (IF) 1:2000 (ICC)	Fitzgerald/70C CR4037GAP	Citrate pH 6.0 n/a
TNNT2	1:500 (FC)	Thermo/MA5-12960	n/a
Ku-80	1:100 (IF)	CellSignaling/2180S	Citrate pH 6.0
Ki-67	1:100 (IF)	Abcam/ab15580	Citrate pH 6.0
Phh3	1:100 (IF)	Abcam/ab5176	Citrate pH 6.0
vWF	1:100 (IF)	Abcam/ab6994	Citrate pH 6.0
Pan-cadherin	1:100 (IF)	Sigma/C3678	Citrate pH 6.0
Caveolin-3	1:250 (IF)	Abcam/ab2912	Citrate pH 6.0
Connexin 43	1:1000 (IF)	Abcam/ab11370	Citrate pH 6.0
CD 03	1:150 (IHC)	Abcam/ab16669	Citrate pH 6.0
CD 20	1:250 (IHC)	BioCare/ACR3004	Citrate pH 6.0
CD45	1:250 (IHC)	Abcam/ab10558	Citrate pH 6.0
CD 31	1:400 (IF)	CellSignaling/3528	Citrate pH 6.0
Cytokeratin	1:50 (IF)	Dako/M3515	Citrate pH 6.0
MLC2 a	1:100 (IF) 1:1000 (ICC)	Thermo/MA5-26390	Tris/EDTA pH 9.0 n/a
MLC2 a	1:750 (FC)	SynapticSystems/311 011	n/a
MLC2 v	1:200 (IF)	BD/565497	Tris/EDTA pH 9.0
MLC2 v	1:300 (FC) 1:500 (ICC)	Abcam/ab79935	n/a
NKX-2.5	1:100 (FC and ICC)	CellSignaling/8792S	n/a

Table S4: List of reagents used in this study.

Reagents	Company	Country	#catalogue
Accutase	Thermo Fischer Scientific	USA	A1110501
Acid Acetic	Êxodo Cientifica	USA	AA09870RA
agarose	Thermo Fischer Scientific	USA	16500500
Alkaline phosphatase polymer kit	Vector	USA	MP-5402
Aniline blue	Êxodo Cientifica	USA	AA09890RA
aqueous slide mount solution	Vector	USA	H-5501
Ascorbic Acid	Sigma-Aldrich	USA	4403
Avidin-biotin complex	Vector	USA	S -2001
B27	Thermo Fisher Scientific	USA	17504044
B27 minus insulin	Thermo Fisher Scientific	USA	A1895601
BMP4	R&D Systems	USA	341-BP-050
Bouin fixative solution	Êxodo Cientifica	BRA	FB08835SO
BSA	Sigma-Aldrich	USA	A2153-100
CHIR99021	Merck Millipore Sigma	USA	361571
Collagenase II	Sigma-Aldrich	USA	17101015
Cyclosporine A	Sigma-Aldrich	USA	30024
Cyclosporine A Sandimmun	Novartis	SWZ	945570
DAB	Vector	USA	SK4105
DAPI	Thermo Fischer Scientific	USA	D1306
Dispase	Sigma-Aldrich	USA	D4693
Donkey serum	Millipore	USA	S30
Essencial8	Thermo Fisher Scientific	USA	A1517001
Ethanol	Cirurgica Estilo	BRA	13462
Fetal Bovine Serum	Thermo Fisher Scientific	USA	12657029
GeITREX	Thermo Fischer Scientific	USA	A1413302
Glucose	Sigma-Aldrich	USA	G8270
Hematoxylin	Êxodo Cientifica	USA	HH09490SO
Hoechst	Sigma-Aldrich	USA	14533
IGF-1	PeptoTech	USA	AF-100-11
KY2111	Cayman Chemical	USA	14315
PBS	Thermo Fischer Scientific	USA	21600-044
PFA	LabSynth	BRA	P1005.06.AG
Picric acid	Imbralab	BRA	4283
Red chromagen	Vector	USA	SK5100
RPMI 1640	Thermo Fisher Scientific	USA	11875093
Saponin	Sigma-Aldrich	USA	84310
Sirius red	Êxodo Cientifica	BRA	SR07371RA
StemFlex	Thermo Fisher Scientific	USA	A3349301
Triton X-100	Sigma-Aldrich	USA	T8787
Trueview (Autofluorescence quenching)	Vector	USA	SP-8400
Tween 20	Sigma-Aldrich	USA	P1379-100
VectaShield	Vector	USA	H1700
Wizard Genomic DNA purification Kit	Promega	USA	A1120
XAV939	Cayman Chemical	USA	13596
Xylol	Êxodo Cientifica	BRA	X09709RA
Y-27632	Cayman Chemical	USA	10005583

Supplementary Figures

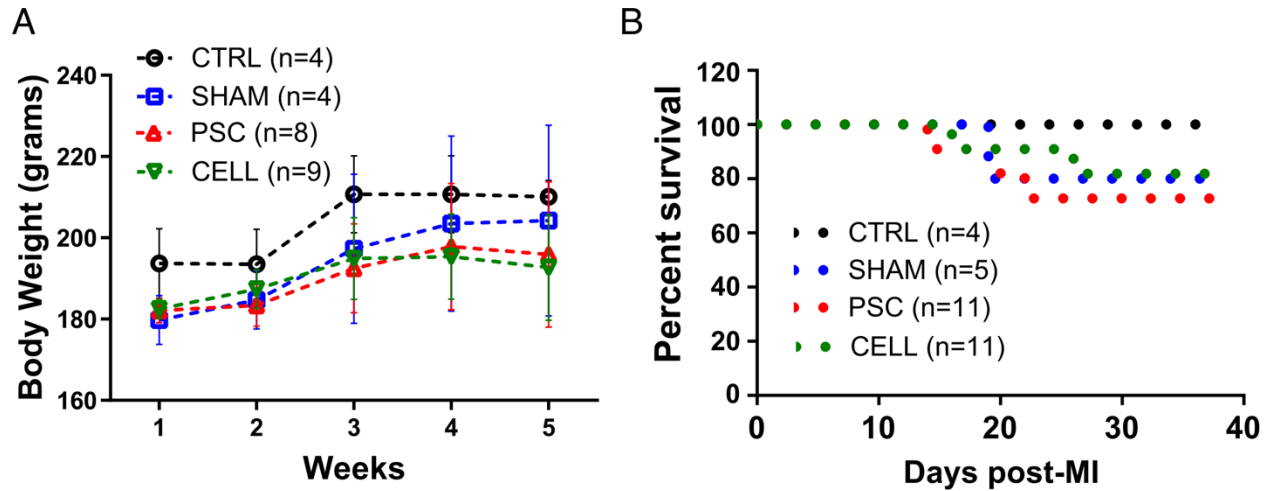


Figure S1: Bodyweight control and survival rate of CsA immunosuppressed and infarcted rats that completed the experimental protocol.

A) The immunosuppression with Ciclosporin A was adjusted weekly based on the animal's body weight, as well as the potential toxicity of the treatment.

B) Kaplan-Meier survival curve. We did not observe any significant difference in mortality/survival.

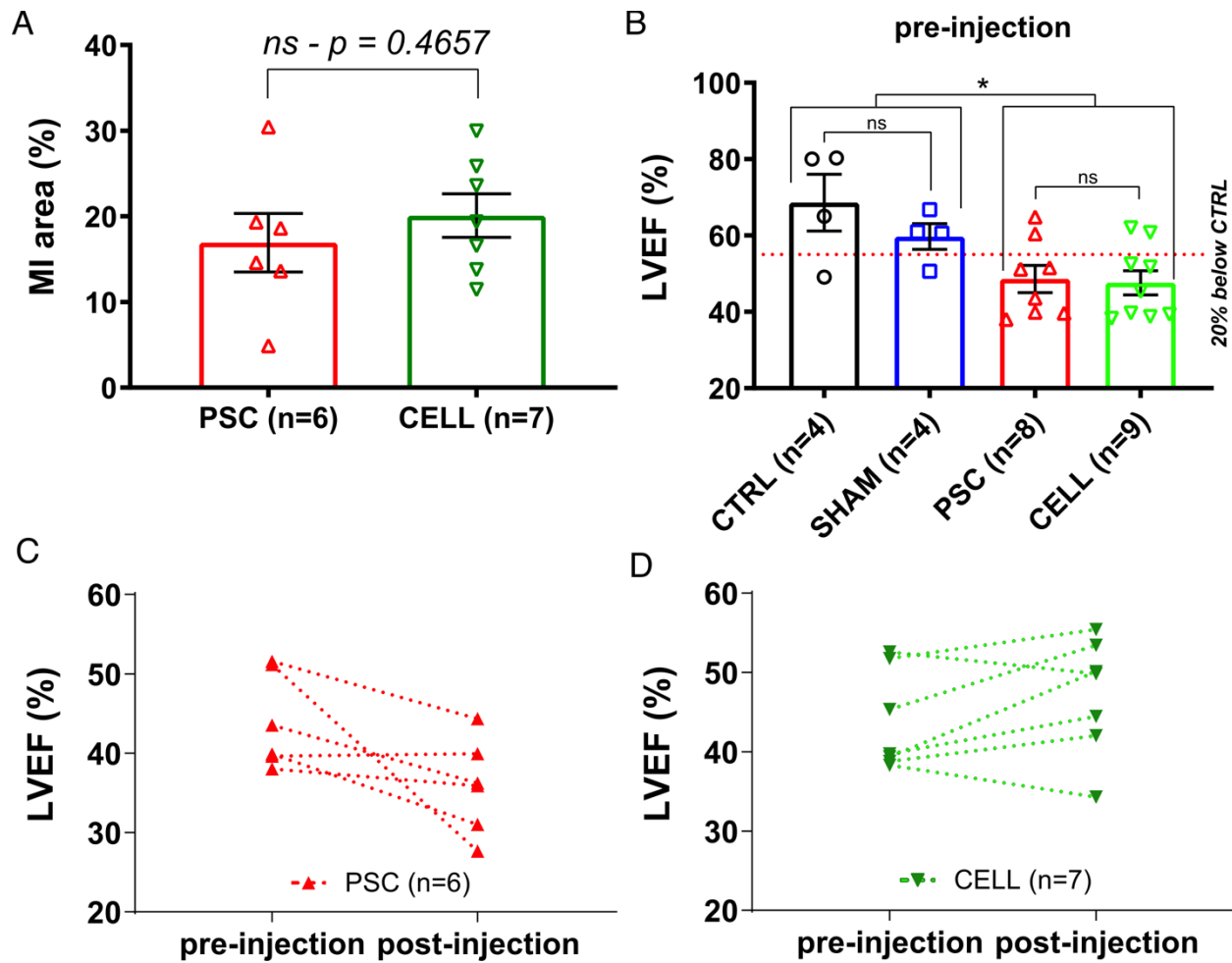


Figure S2: MI area and LVEF pre-injections. Functional improvements can be associated with the identification of human grafts into the fibrotic scar. Picrosirius red-stained representative cross-sectional images were used to quantify the percentage of MI area 30 days after treatment.

A) Quantification of MI area (mean \pm SE). **B)** Animals that completed the experimental therapy had their LVEF pre-treatment used to exclude rats without significant impairment of cardiac function. The red dashed line represents the pre-treatment limit for animals to be considered in the next steps of analysis. This threshold was calculated based on the mean LVEF of the CTRL group subtracting 20% of this value to establish the cut-off. Note that 2 rats from the PSC group and 2 from the CELL group are above the limit. These 4 animals were excluded from the next set of functional and molecular assessments. Pre-injections both couples CTRL and SHAM and PSC and CELL animals displayed similar LVEF. Also, as expected PSC and CELL rats showed deteriorated LVEF compared with CTRL and SHAM animals. $P < 0.05$. **C)** LVEF values Pre- and post-injection for each animal from the PSC group. **D)** LVEF values Pre- and post-injection for each animal from the CELL group.

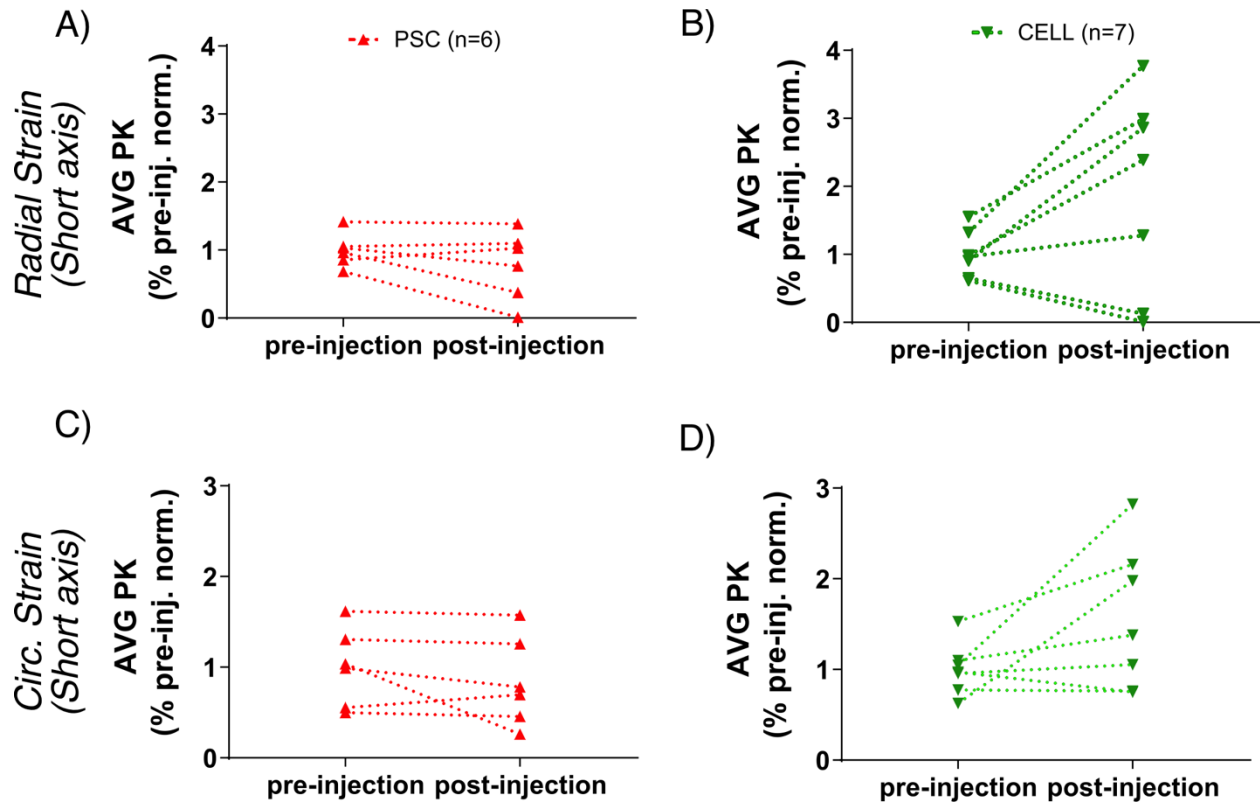


Figure S3: Short Axis Strain Analysis. Radial and circumferential strain time-to-peak were calculated using papillary level images and the average time-to-peak (AVG PK) for all the six segments normalized by mean pre-injection values for each group to access how treatment modulated this parameter. **A)** Radial Strain time-to-peak (AVG PK) of PSC rats normalized by pre-treatment values. **B)** Radial Strain time-to-peak (AVG PK) of CELL rats normalized by pre-treatment values. **C)** Circumferential Strain time-to-peak (AVG PK) of PSC rats normalized by pre-treatment values. **D)** Circumferential Strain time-to-peak (AVG PK) of CELL rats normalized by pre-treatment values.

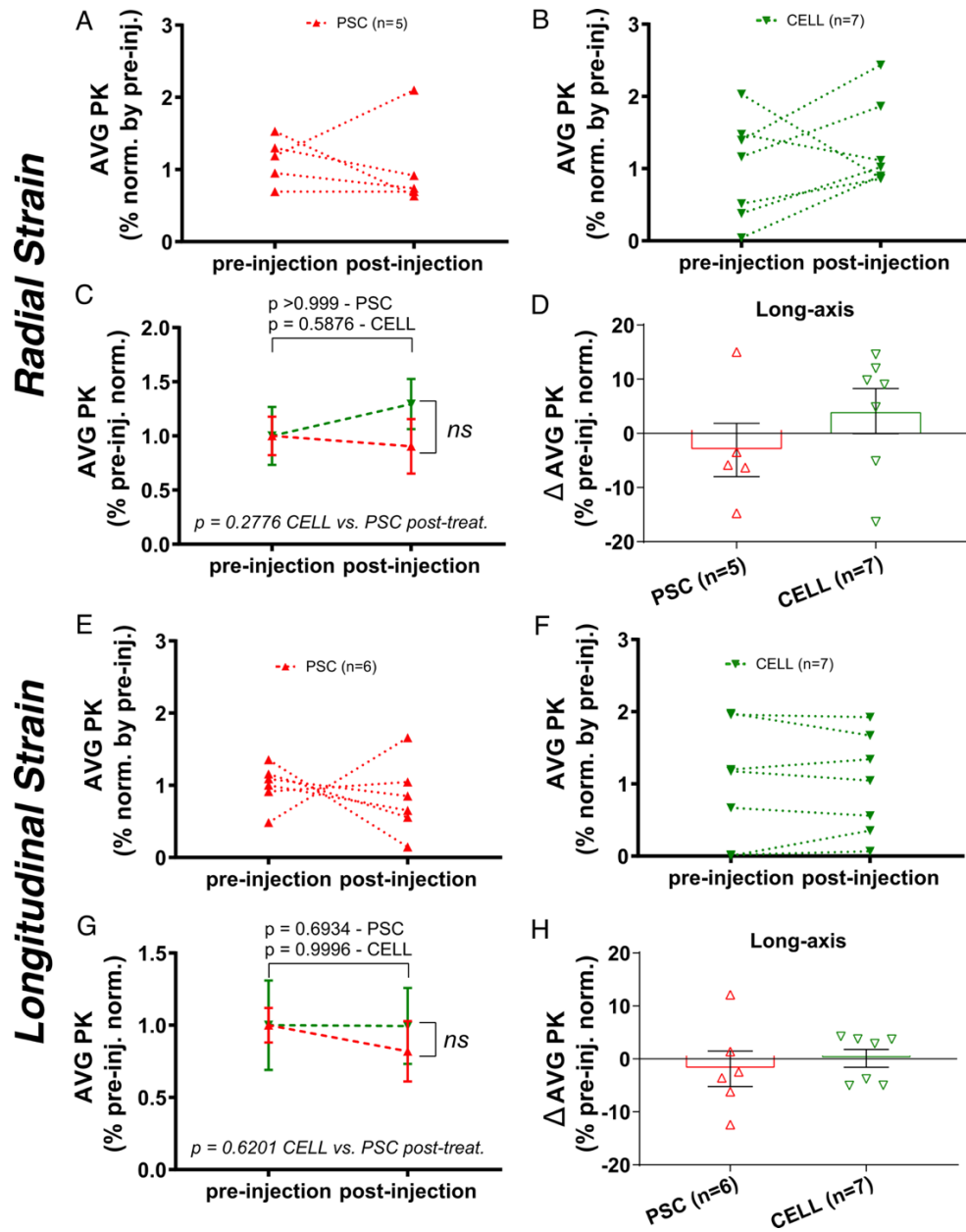


Figure S4: Long Axis Strain Analysis. Radial and longitudinal strain time-to-peak were calculated using longitudinal mid-portion images and the average time-to-peak (AVG PK) for all the six segments normalized by mean pre-injection values for each group to access how treatment modulated this parameter. **A)** Radial Strain time-to-peak (AVG PK) of PSC rats normalized by pre-treatment values. **B)** Radial Strain time-to-peak (AVG PK) of CELL rats normalized by pre-treatment values. **C)** Mean Radial Strain time-to-peak (AVG PK) of PSC and CELL rats were normalized by their respective pre-treatment values. **D)** Radial Strain time-to-peak delta post-minus pre-injection. **E)** Longitudinal Strain time-to-peak (AVG PK) of PSC rats normalized by pre-treatment values. **F)** Longitudinal Strain time-to-peak (AVG PK) of CELL rats normalized by pre-treatment values. **G)** Mean Longitudinal Strain time-to-peak (AVG PK) of PSC and CELL rats were normalized by their respective pre-treatment values. **H)** Longitudinal Strain time-to-peak delta post- minus pre-injection.

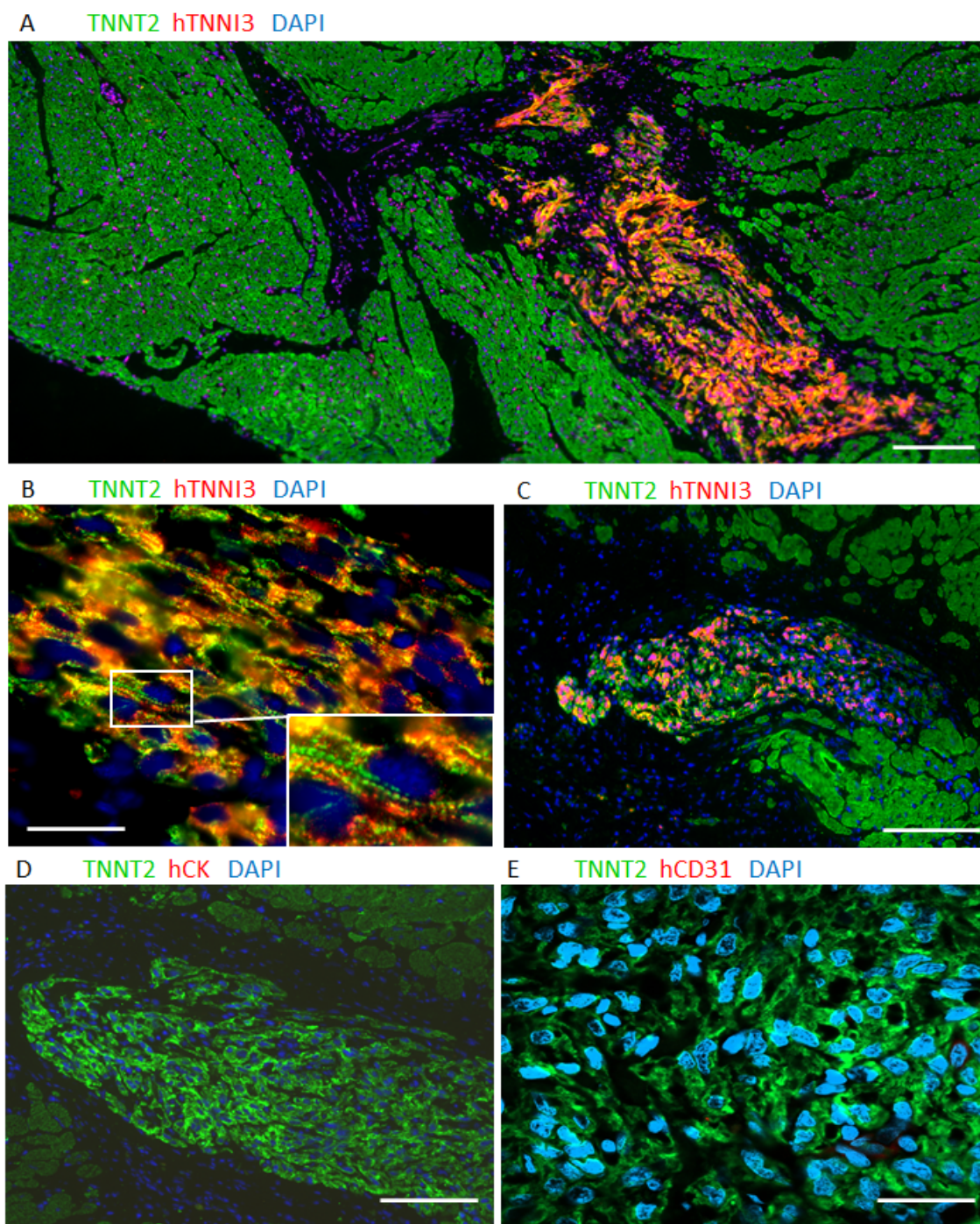


Figure S5: Morphology of the human graft. **A)** location of the graft in rat tissue marked for hTNNI3 (red), TNNT2 (green), and nuclei (blue). **B)** High magnification of TNNT2 and hTNNI3 double-positive cardiac human tissue showing sarcomere organization in detail. **C)** Another

example of human graft expressing TNNT2. **D**) No red staining for human CK. **E**) No-expression of human endothelial cells positive for CD31. Scale bar: 50 μ m.

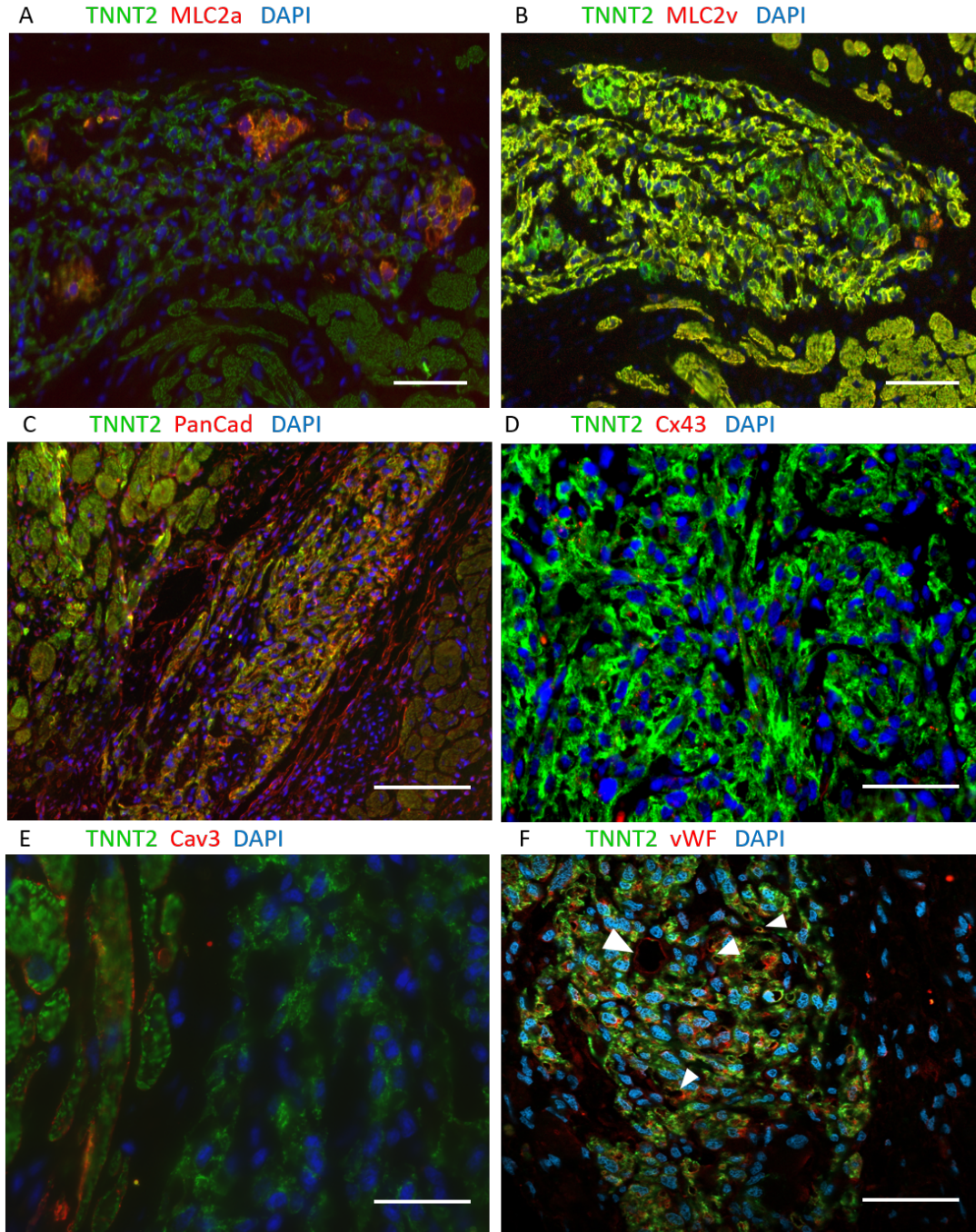


Figure S6: Maturation and cell-cell interaction in the human graft by immunofluorescence staining. **A**) Co-staining for TNNT2 (green) and MLC2a (red), nuclei were counterstained with DAPI (blue). **B**) Immunostaining for MLC2v and TNNT2 with DAPI in the same graft marked with MLC2a (A). General cardiac marker TNNT2 (green) and red subtype marker Pan-Cadherin

(C), Connexin 43 (D), Caveolin 3 (E) and vWF (F) with arrowheads show vascularization within the graft. Scale bar: 50 μ m.

TNNT2 Pan Cadherin Nuclei

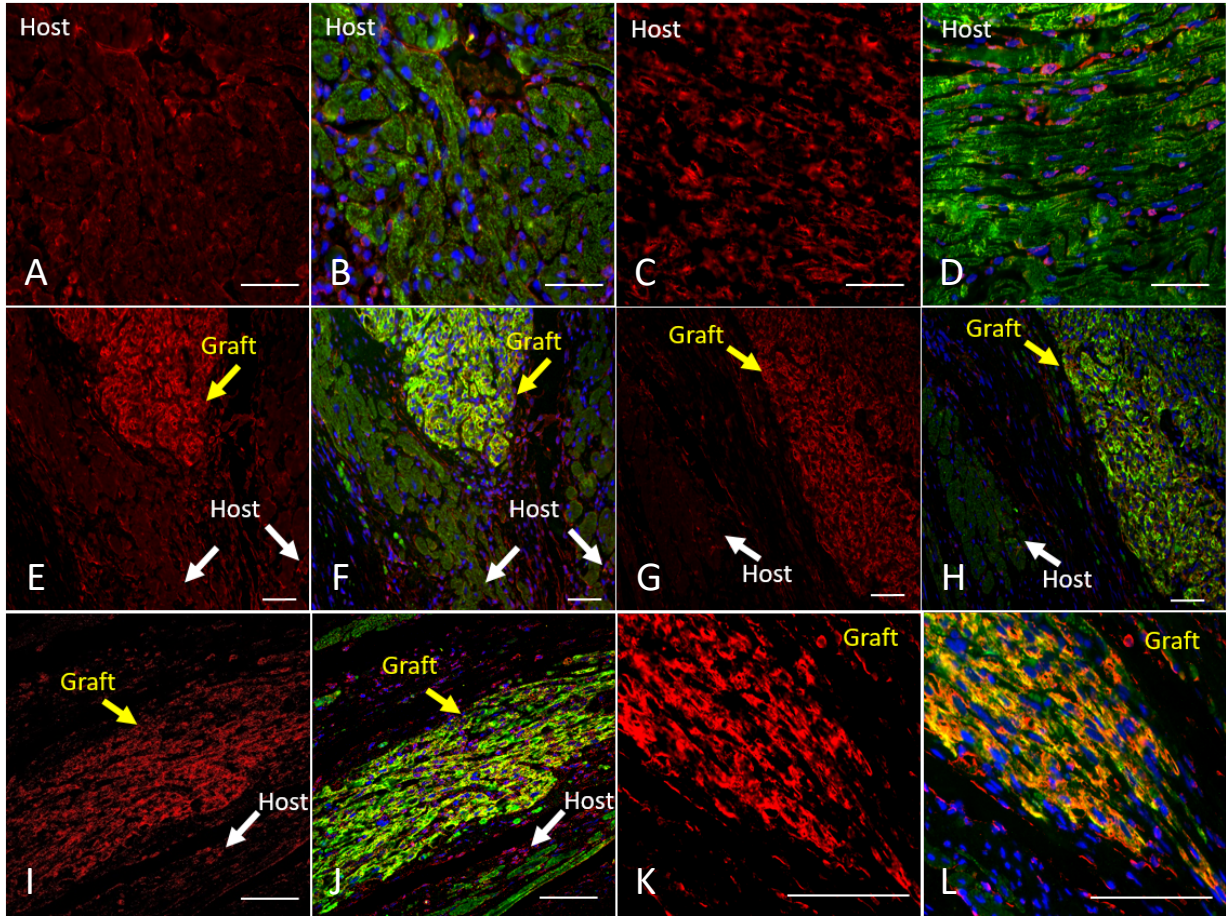


Figure S7: *Immunofluorescence staining for TNNT2 and Pan-cadherin.* Immunofluorescence staining for TNNT2 and Pan-cadherin showing host and graft labeling in different cell-treated rats. White arrows indicate rat heart muscle and yellow arrows show human grafts. The expression of Pan-cadherin stronger at cell borders and structured in the host tissue. Conversely, the human graft displays higher intensity of Pan-cadherin without a clear structured organization. Note that hiPSC-CMs composing the graft are clearly smaller and randomly organized as a tissue compared with host muscle. Clearly, Pan-cadherin is expressed in the interphase host/graft border, strongly suggesting coupling. A, B, E-L) Animal 29, C-D) Animal 39. Scale bars: 50 μ m.

TNNT2 Cx43 Nuclei

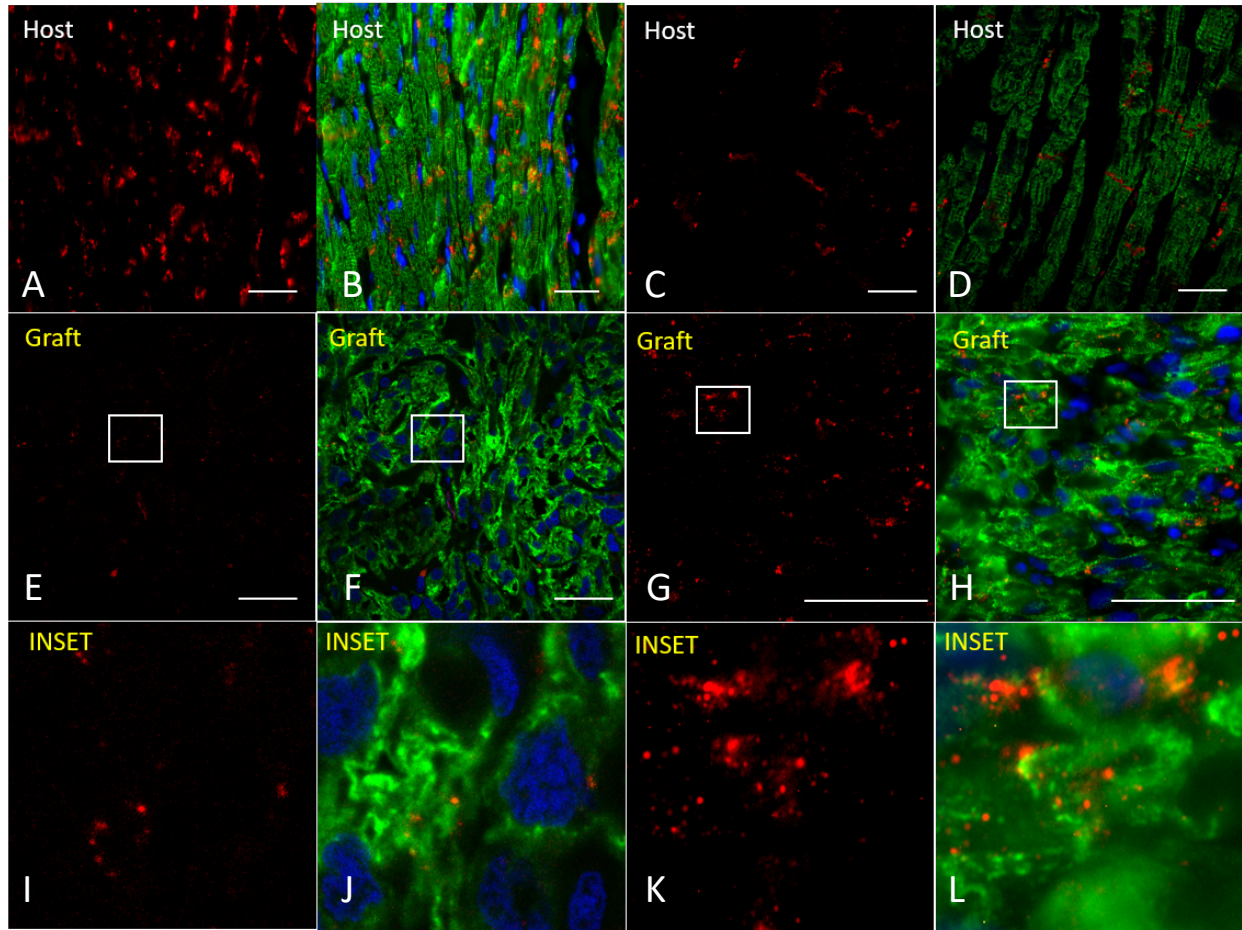


Figure S8: *Immunofluorescence staining for TNNT2 and Cx43.* Immunofluorescence staining for TNNT2 and Cx43 showing broader labeling for Cx43. Note that the expression of Cx43 is highly structured specially in the short borders of adult cardiomyocytes. Conversely, Cx43 is scant and less structured into the grafts. Note the smaller sizes of hiPSC-CMs compared with adult cardiomyocytes (bottom images, host tissue). The random organization of hiPSC-CM grafts also impair the visualization of cell borders and Cx43 expression. **A-B)** Animal 45, **C-F and I-J)** Animal 29, **G-H and K-L)** Animal 39. Scale bars: 50 μ m.

TNNT2 Caveolin 3 Nuclei

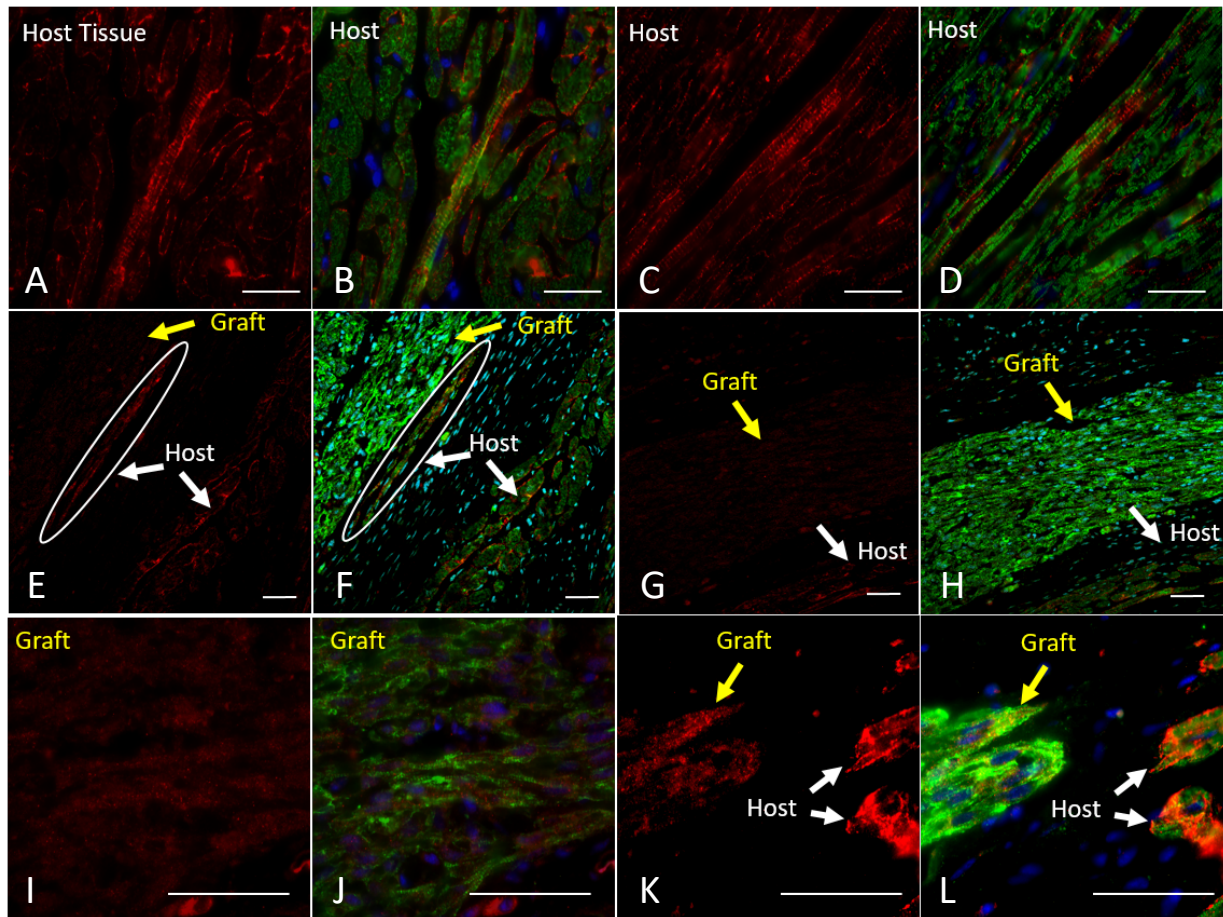


Figure S9: *Immunofluorescence staining for TNNT2 and Caveolin 3.* Immunofluorescence staining for TNNT2 and Caveolin 3 showing an evident structure and intense labeling of adult cardiomyocytes and scant and random labeling into the human grafts. hiPSC-CMs express Cav3, but the intensity and the organization commonly observed in adult cells were not reached in the time frame of these analyzes. Clearly, Cav3 is expressed in the interphase host/graft border, strongly suggesting coupling. **A-B and E-H)** Animal 29, **C-D)** Animal 31, **I-J)** Animal 39. Scale bars: 50 μ m.

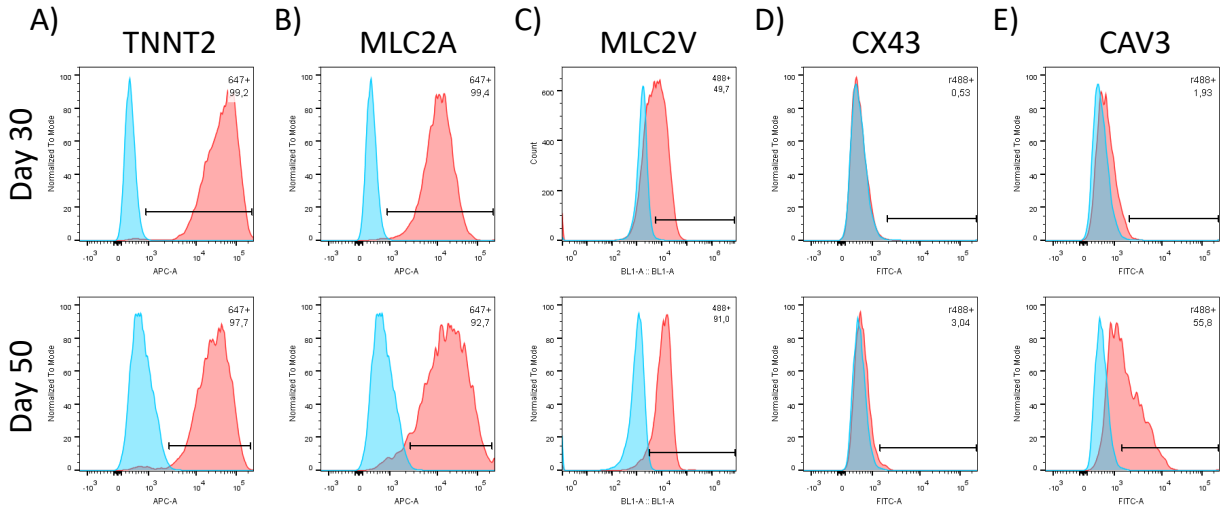


Figure S10: Flow Cytometry quality-control analysis for monitor hiPSC-CMs maturation over time. We performed Flow Cytometry assessments to measure the percentage of positive cells expressing cardiac markers on days 30 and 50 in culture (after the beginning of the differentiation). **A)** Cardiac cells were defined by the expression of troponin T2 (gene symbol TNNT2). **B)** The percentage of positive cells expressing the atrial MLC2a (and a marker of immature hiPSC-CMs) was never down-regulated in vitro. Conversely, **C)** the expression of ventricular MLC2v significantly increases over time. **D)** The expression of Cx43 was not enhanced even after 50 days in culture. **E)** The expression of Cav3 was boosted only partially on day 50. All the antibodies were validated using negative and positive control cells, and they are routinely used in our lab to assess the standards for cardiomyocytes' production. In blue, isotypic antibodies were used to define negative staining, according to the protein-specific antibodies used.

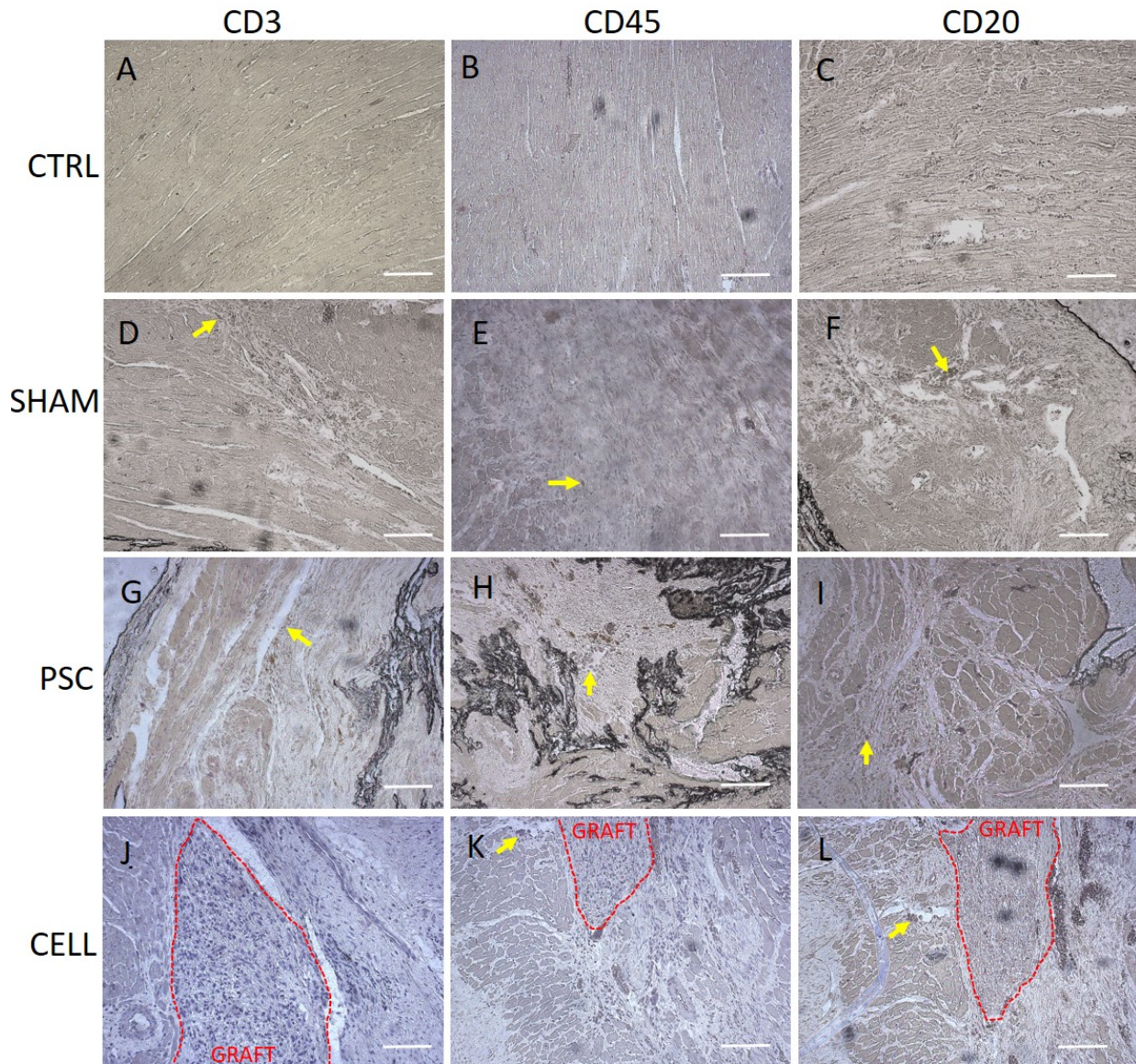


Figure S11: *Immunohistochemistry for inflammatory markers.* A-C No evidence for CD3, CD45 and CD20 respectively, in the healthy control group. D-F) Diffuse labeling for CD3, CD45 and CD20 in the SHAM group. PSC group shows diffuse (G; I) and patchy (H) labeling for all markers. The CELL group shows no evidence for CD3 labeling (J) but shows patches of CD20 and CD45 markers (K-L). Yellow arrows very small groups of inflammatory cells. Scale bar: 50 μm .

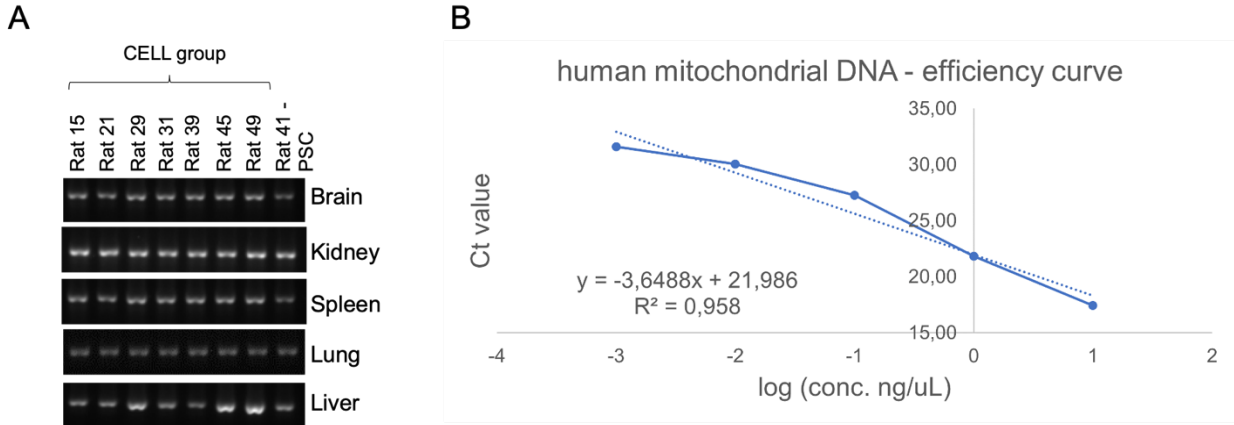


Figure S12: *Human mitochondrial DNA was identified in some tissues other than the heart and subjected to qPCR analysis. A)* Rat DNA sequence was amplified as a control for reactions. **B)** Quantitative human mitochondrial DNA. Standard curve of human mitochondrial DNA sequence in 1pg, 10pg, 100pg, 1ng, and 10ng of human DNA diluted in 200ng of rat DNA per sample. We considered 1pg of human DNA our lowest detectable amplification.

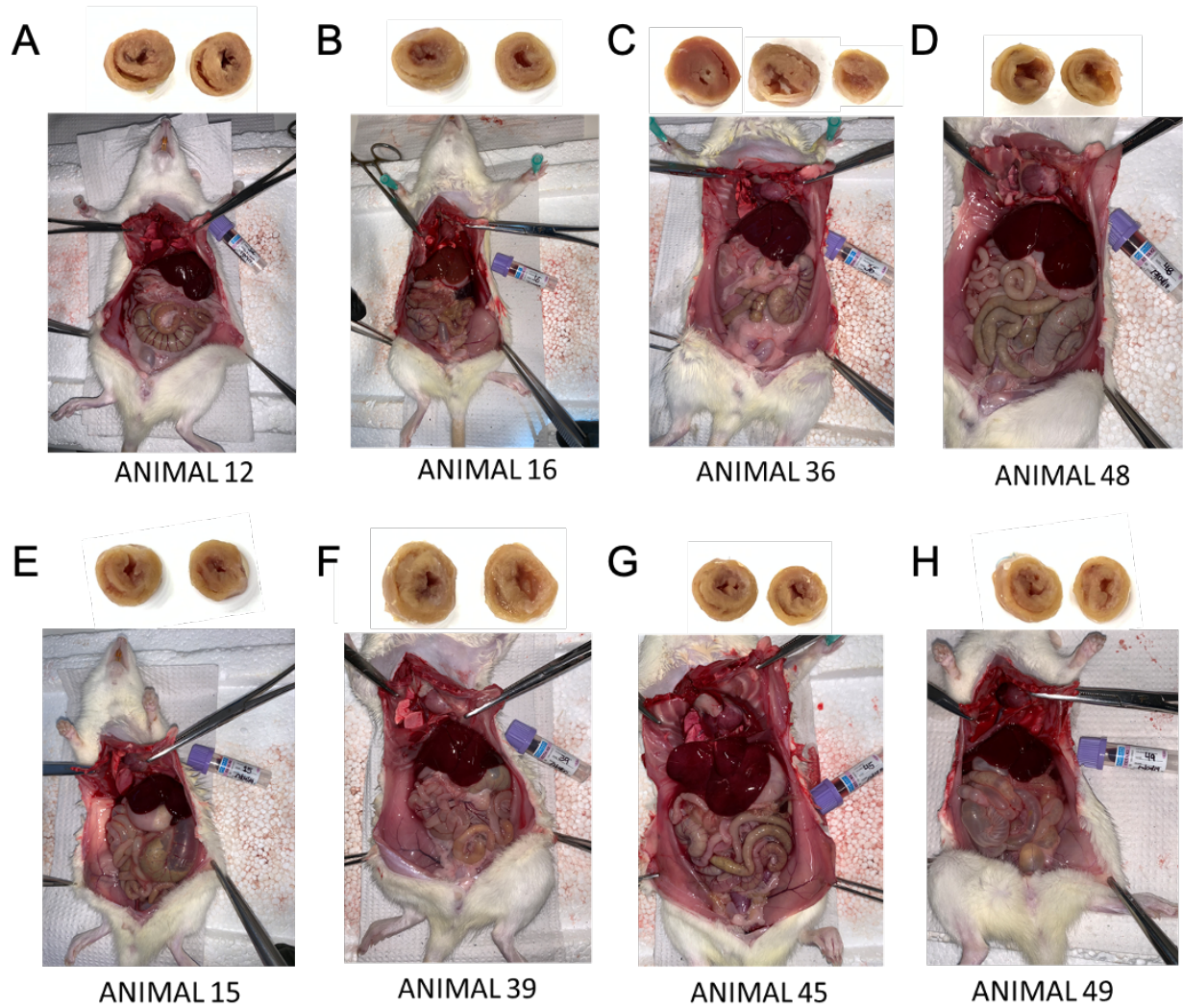


Figure S13: Necropsy. On day 37, rats that underwent deep anesthesia were euthanized by the direct injection of KCl overdose. **A)** Healthy control rat. **B)** SHAM rat. **C and D)** PSC rats (MI-induced animals). **E-H)** CELL-treated rats (MI-induced) whose human DNA was found out of the heart.